ISSN 0016-8521, Geotectonics, 2015, Vol. 49, No. 5, pp. 411–424. © Pleiades Publishing, Inc., 2015.
Original Russian Text © A.V. Marinin, L.A. Sim, 2015, published in Geotektonika, 2015, No. 5, pp. 62–77.

The Contemporary State of Stress and Strain at the Western Pericline of the Greater Caucasus

A. V. Marinin and L. A. Sim

Schmidt Institute of Physics of the Earth, Russian Academy of Sciences, ul. Bol'shaya Gruzinskaya 10, Moscow, 123995 Russia
e-mail: marinin@ifz.ru

Received April 14, 2014

Abstract—We collected materials on geological indicators of paleostresses at the western pericline of the Greater Caucasus mega-anticlinorium and within the large transverse flexure-fault zone (Anapa and Dzhiginka zones) limiting this mega-anticlinorium. Based on the data, we reconstructed local stress states in different tectonic zones. The reconstructed local stresses showed a considerable variation of the orientations axes of principal stress near the two zones. In a site adjacent to the flexure-fault zone and located near the western pericline of the Greater Caucasus mega-anticlinorium, the detachment systems of northeastern (NE–SW) strike are determined. Additionally, field structural studies proved elongation in the northwestern (NW–SE) direction. This was also verified by the reconstruction of orientations of minimum compression stress axes (maximum deviatory tension) implemented by cataclastic analysis of structural–kinematic information on the movements of the fault planes (tectonic cracks and minor ruptures). We found a well-expressed multistage regime of the northwestern (NW–SE) tension within the limits of the Semisam anticline. Tension deformations (along the axis of the main folded structure) are manifested in structures of different scales; the values of relative elongation are defined for some of them. At the western pericline of the Greater Caucasus mega-anticlinorium, in the Miocene deposits, a north–south (NNW) compression regime with steep inclinations of axes of maximum compression stresses was identified. In the boundary zone between the Northwestern Caucasus and transverse Kerch–Taman trough, an alteration of the orientations of main axes of normal stresses was found. These changes led to the replacement of horizontal-compression and horizontal-shear (with a NE-oriented compression) settings, which are predominant in the Caucasus, with settings of horizontal tension (with steep NNW-oriented compression axes).

Keywords: stress field, local stress state, structural paragenesis, slickensided surfaces, detachment

DOI: 10.1134/S0016852115040068

INTRODUCTION

When studying folded deformations in the Greater Caucasus, the main focus is usually placed on the orientation of shortening across the folded structure (i.e., in the direction where the major part of the easily detectable horizontal shortening is located). In the Western Caucasus, different researchers (A.L. Kozlov [6], M.V. Muratov [13], Ch.B. Borukaev [2], V.E. Khain [12, 27], E.E. Milanovskii [12], A.N. Shardanov [28], L.M. Rastsvetaev [19, 21, 22], T.V. Giorgobiani [4], F.L. Yakovlev [31, 32], A.M. Nikishin [15], and others) have established a considerable influence of, or a leading role played by, horizontal shortening in the southwest–northeastern direction, in forming the tectonic structure of the region. Despite the long-term period of these studies, there have been different approaches to the causes and parameters of this shortening. In the authors' opinion, the problem regarding the source of driving forces for horizontal shortening, and that regarding the relationship between and directions of relative horizontal and vertical displacements, can be solved by methods of field tectonophysics. In the Greater Caucasus, which is traditionally a test area for Russian tectonic researchers, many studies have been implemented by various methods. The western part of the Caucasus has been studied in many works (for example, [3, 4, 7, 9, 11, 14, 16, 19, 21, 22, 34, 35] and others) by using different structural tectonophysical methods.

On the basis of study of the faults in the region, L.M. Rastsvetaev has formulated ideas on the folded structure of Northwestern Caucasus: he suggests this region is a transpressive right-lateral strike-slip fault zone [19]. The state of the lithosphere within the limits of Mountain Crimea (Gornyi Crimea) and Northern Cis-Black-Sea Region during the Alpine tectonic epoch was characterized by an submeridional shortening (stresses of maximum deviatory compression) and a reactive elongation (stresses of maximum deviatory tension) in the sublatitudinal or subvertical directions. The mobilization of NW- and NE-oriented inhomogeneities, both those newly formed and already existing by the beginning of the Alpine cycle, has determined a broad distribution of deformations related to

strike-slips, predominantly NW-oriented right-lateral strike-slips [19].

The character of the lineament network and macrocracking in the Western Cis-Caucasus Region has been considered by V.A. Viginskii [3]. The data on cracking in the northern part of the Taman Peninsula from this work agree with the observed lineament network in that territory. Based on the analysis of structural parageneses, the cited author has established the NNW (340°–350°) orientation of the axis of maximum compression stresses and the NE (70°–80°) orientation of the intermediate axes of principal stresses.

Characterizing the field of tectonic stresses in the area of the Inguri Hydroelectric Power Plant, P.N. Nikolaev focused [16] on the change in the main characteristics of the stressed state when transiting from one geostructural element to another (fold hinges and limbs, ruptures). The localization of different types of stress fields within the limits of different structural elements indicates, in the opinion of the mentioned author, the localization of strains within these structural units.

Based on the study by T.V. Georgobiani and D.P. Zakarai aimed at discovering how the Alpine structures of the region were formed, the characteristic zonation in the cross section, namely consecutive change in folding from moderate to weak in the SW to NE direction, was verified. Within the limits of the southern slope of the Northwestern Caucasus, interference-folded structures were found; these structures developed when the folding waves from two directions overlapped. The leading role in emplacement of the contemporary folding structure was played by the SW–NE-directed tangential forces appearing as a result of underthrusting of the Black-Sea–Transcaucasian central massif beneath the folded structure of the Greater Caucasus. These authors also supposed a change in the direction of the lateral deformation pattern from northeastern to submeridional during the Alpine cycle development of the folded structure [4].

A study by S.A. Nesmeyanov, using a technique of structural–geomorphologic analysis of neotectonic structures, allowed him to conclude the following. The mountainous structure of the Northwestern Caucasus was formed during the entire neotectonic stage, inheriting the late-geosyncline highs with its near-axial part. The mega-arch of the Greater Caucasus is a part of the Crimean–Caucasian range of the orogenic mega-anticlinoria; within the limits of this range, the Greater Caucasus is divided from the Crimean mega-anticlinorium by the Kerch–Taman saddle-like zone, which was a deep transverse molasse-filled trough at the early orogenic stage. At the end of the late orogenic stage, this zone was involved into the uplift oriented in a direction transverse to the axis of this early orogenic trough, and this uplift formed a united range of neotectonic megarise. To choose a neotectonic and contemporary tectonic–dynamical setting, one should take into account the broad distribution of structures whose formation is related to the longitudinal and transverse tension of the Greater Caucasus mega-anticlinorium [14].

With the help of a structural–geomorphologic method for reconstructing shear stresses [25], neotectonic stresses of the Northern Cis-Caucasus Region were inferred [8]. Based on the interpretation of feathering faults in the zones of dynamical influence of the Akhtyrka W–NW-trending fault zone, the NNW-oriented horizontal compression axes and the conditions of additional tension in this fault zone near the Greater Caucasus pericline were reconstructed. The neotectonic stresses were reconstructed on the basis of analysis of the feathering faults manifested among the Miocene–Pliocene deposits of the Scythian Plate.

Studies carried out in 1995–2007 by the tectonic-dynamic group of researchers leaded by L.M. Rastsvetaev at the northwestern pericline of the Novorossiysk synclinorium and the Psebe anticline zone have revealed structural parageneses related to three main subhorizontal directions of the maximum compression stresses: northeastern, northwestern, and submeridional [11, 21, 22, 34]. The northeastern compression caused the development of structural parageneses that formed during folding and agreed with the orientation of the large folded structures of the Novorossiysk synclinorium (maximum compression is oriented orthogonally to these structures). The northwestern (to NNW) orientation of the maximum compressing stresses noticeably dominates in the Miocene–Pliocene deposits [11, 34]. According to the mentioned study, the meridional orientation of the maximum compression stresses within this area is weakly manifested, in contrast to areas located to the east, within the limits of the Northwestern Caucasus.

The interrelation between the Late Cenozoic stresses and deformations in the Caucasian sector of the Alpine belt and in the cratonic zones framing this belt was studied by the group of researchers with the use of the structural–paragenetic method and tectonic stress monitoring [9]. They found a united stress and strain field were caused by the convergence of the Arabian and Eurasian plates, and proposed a model of a longitudinal wave strain mechanism that would explain the spatial and temporal change in the main parameters of the reconstructed stress field. For the rocks within the axial zone of the Caucasus, which is distinguished on the basis of the character of Alpine deformations, relative shortening is up to 50–80% in places, while elongation is more than doubled [9].

French researchers determined 14 local stress states at the western pericline of the Greater Caucasus, that were analyzed in the context of the tectonic evolution of the region [35]. The local stress states for the entire region of Northwestern Caucasus (123 values), having the same characteristics (orientations of axes of principal stresses, type of stress state), were grouped into tectonic regimes. As a result, quite homogeneous

paleostress fields were defined for the entire studied region; moreover, certain tectonic settings were chosen for each of these fields on the basis of earlier paleotectonic reconstructions and models. For these tectonic settings, common general orientations of stresses were supposed, as well as a common type of stress–strain state and a united formation time. Based on these ideas, ten paleostress fields were distinguished for the entire region of Northwestern Caucasus from the Late Cretaceous. In the context of the present work, of the most interest are the pre-Eocene regimes of horizontal tension with sublatitudinal (to ENE–WSW) and NW–SE orientations of the axis of main deviatory tension, and the post-folding regime with the NNE–SSW-oriented axis of main deviatory tension [35].

F.L. Yakovlev estimated the possible extent of shortening for the Northwestern Caucasus across its folded structure: the relative shortening for the western cross section (Abrau–Dyurso) was 16% [31]. For the elongated folded structures, he assumed an absence of possible regional shortening or elongation deformations along the fold axes [32]. Therefore, the average shortening for each of the considered cross sections will be oriented across the folded structure, while elongation takes place in the vertical direction.

GEOLOGICAL OVERVIEW

At the western pericline of the Greater Caucasus, the main tectonic structures are represented by the terminal northwestern segment of the Novorossiysk synclinorium and the Psebe anticline zone located north of the synclinorium (Fig. 1). The Lower Cretaceous deposits are exposed in the northeastern part of the Novorossiysk synclinorium, while the Upper Cretaceous and Paleogene ones are exposed in its southwestern part. The Lower Cretaceous deposits are represented mostly by argillic rocks intensively involved in mud volcanism and the diapir-like structures of some folds in the considered region. The Upper Cretaceous part of the section is composed of rhythmical interleaving of predominantly carbonate rocks (limestones, argillic limestones, limy clays) with the subordinate amount of terrigenous rocks (sandstones, siltstones, and clays). The Paleogene deposits are represented by rhythmical interleaving of mostly terrigenous rocks. The rocks in the lower part of the Paleogene age are often highly silicified. The main folded structures of the Novorossiysk synclinorium and the Psebe anticline zone were formed in the Late Eocene–Miocene [1, 14, 30]. The Maeotian–Pliocene deposits overlie this folded structure with an angular unconformity.

The Kerch–Taman transverse trough is located northwest of the Caucasian folded structures. It is composed of a thick succession of Neogene–Quaternary deposits. The folded structures of the Kerch–Taman trough started to form in the Sarmatian, according to the evidences of synsedimentation folding [29]. The syncline cores that contain Pliocene–Quaternary rocks were relatively recently exposed on the surface. Contemporary signs of the fast tectonic uplift can be observed at Cape Kamennyi [18], where a fragment of the sea floor rose above the sea level for a short time interval (from a day to a month, based on the evidence of different eyewitnesses).

INITIAL DATA AND AIMS OF THE STUDY

In 2011–2012, the authors collected information on the distribution of geological indicators of paleostresses at 64 points during field studies at the western termination of the Greater Caucasus and in the adjacent Kerch–Taman trough (Fig. 1). The total number of measurements (tectonic cracks, slickenside surfaces, detachments, veins, and so on) is about 800. Owing to the layered structure of the sedimentary strata of the Northwestern Caucasus and the different composition of layers, the obtained data are highly valid, because, in addition to the direction inferred from sliding traces, the amplitude of relative displacements for walls of fine faults was also measured in many cases. During field studies, attention was paid to the chronological and structural–paragenetic analysis of the studied faults and folds.

The main aim of the present work was to identify the character of the change in the parameters of the stress–strain state, especially along the orientation of the folded structure. Another aim was to determine the relationship between tectonic structures related to the settings of northeastern and northwestern shortening.

METHODS

When studying the geological indicators of paleostresses of different scales, a structural–paragenetic analysis of ruptures was used [20]. This method utilizes three categories of geological indicators of tectonic stresses/strains: (1) tension-related faults (detachment ruptures, veins, dikes); (2) compression-related faults (foliation and cleavage planes, stylolite sutures); (3) shear faults (the mechanical sense is used intentionally here) including, strike-slips, normal and reverse faults, thrusts, and nappes. Indicators of the first category allow us to find the position of axis of maximum deviatory tension/elongation and, less reliably, that of maximum compression/shortening. Structures of the second category, in contrast, help find the orientations of maximum compression/shortening axes. Revealing the characteristic parageneses of ruptures corresponding to a certain type of stress-strain state can be correct if the indicators of tectonic stresses are geologically coeval and belong to structural elements of the same rank. To process the obtained measurements on ruptures with the found kinematic displacement type, we used the cataclastic analysis (CA) of structural–kinematic data on ruptures [23]. With the use of this approach, we defined the quanti-

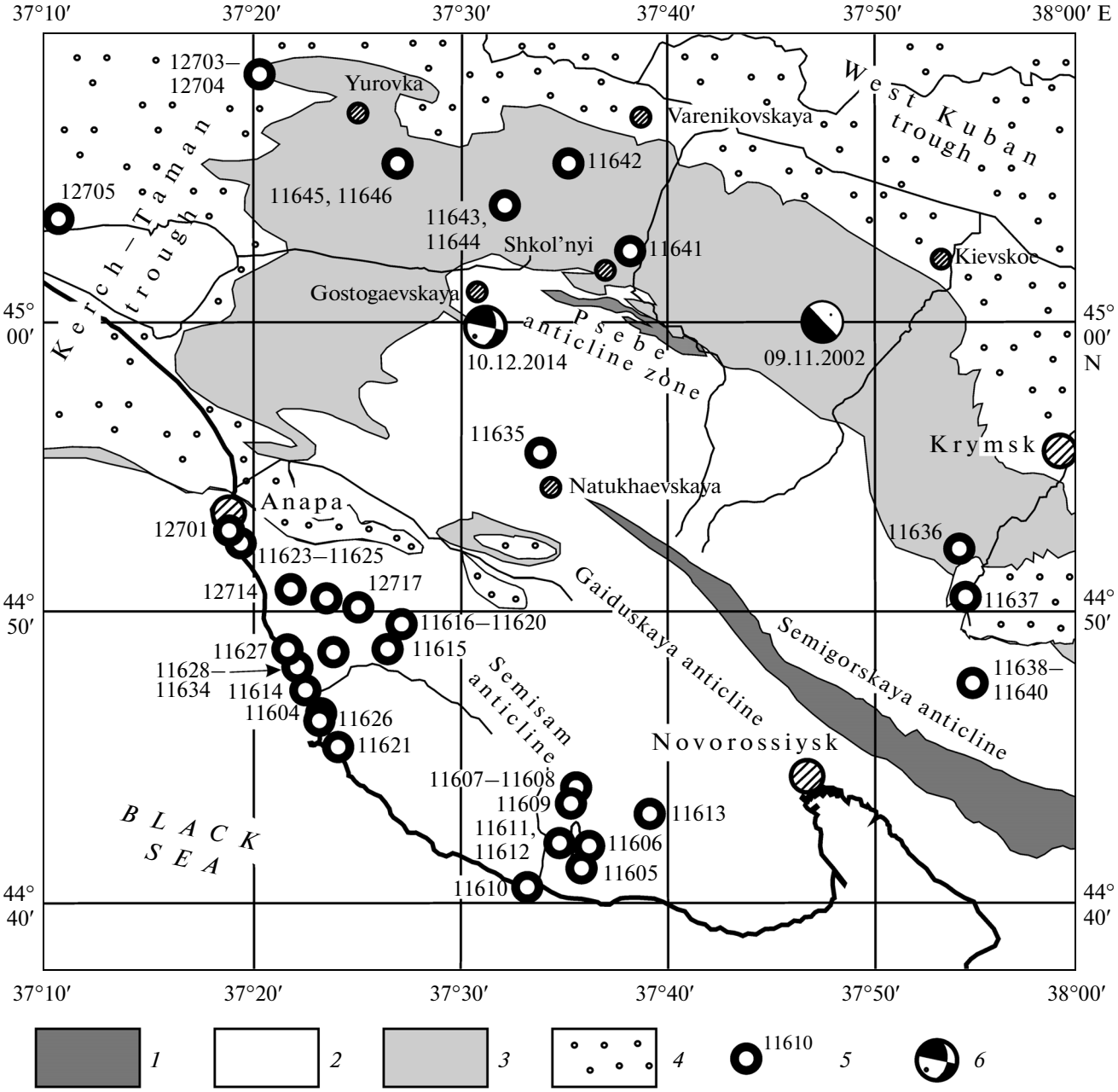

Fig. 1. Locations of the observation points and the main tectonic structures in the studied area, on the basis of the data from [24]. (*1*)–(*4*) deposits: (*1*) Lower Cretaceous (Aptian–Albian), (*2*) Upper Cretaceous–Eocene, (*3*) Maikopian–Neogene, (*4*) Neogene–Quaternary; (*5*) observation points; (*6*) epicenters of large earthquakes.

tative characteristics of local stress states obtained: the positions of principal stress axes and the Lode–Nadai factor. This approach utilizes the general energy statements of contemporary plasticity theory and allows us to calculate both the parameters of stress tensor and those of the quasiplastic deformation increment tensor in the common regime. With this approach applied, values of the spherical and deviatory components of the stress tensor can be measured. The obtained stress tensor characterizes the stress field at any given point—the local stress state—for each studied volume (in the case of field studies, these volumes are observation points). The axes of principal stresses or axes of stress tensor in the classical and structural mechanics have the following indices and names: σ_1, σ_2, and σ_3 are the algebraic maximum (minimum compression stresses or maximum deviatory tension), intermediate, and algebraic minimum (maximum compression stresses or minimum deviatory tension) stresses, respectively, for positive values of tension stresses and negative ones of compression stresses. A stress tensor has spherical and deviatory stress compo-

nents. In the case of a rock massif, the spherical component of a stress tensor can be compared to uniaxial pressure, while the deviatory component agrees with the tectonic stresses leading to observed deformations. For proximate values of two principal stresses, their axes in the rock massif undergo "replacement" or "reindexing" for stress states proximate in the spatiotemporal sense. The main differences of cataclastic analysis from the methods of the dislocation analysis [5, 33] are the parallel calculation of seismotectonic deformation tensor and finding the orientations of the stress tensor's main axes on the basis of the principle of maximum energy dissipation for the set of fractures from a homogeneous sampling.

When analyzing the obtained characteristics of local stress states, we used the technique of determining the "general field" of stresses [26]. Mathematical modeling data on local stress field distribution in the vicinity of a rupture [17] became the basis of this approach and helped to formulate the principle of distinguishing the "general field" of stresses, which averages the regular fluctuations of principal stress axes due to movement of these axes on the rupture. These orientations of axes σ_1 and σ_3, the suffered fluctuations, are joined into compression and tension cones with a 90° angle at the top. Tension axes are not included in compression cones, while compression axes cannot be included in tension cones. Axes of cones are mutually perpendicular and are compression and tension axes of the "general field" of stresses (this field is external relative to the rupture); their tangency points are the poles of sites where maximum tangential stresses act. By using the approach described above, we can find the "general," averaged field for any studied site based on the data on orientations of axes σ_1 and σ_3: depending on the scale of study, the obtained field will be "external" (relative to the studied area), or "regional" (if the area is quite big and includes several tectonic structures). In the case where all local compression and tension axes are insufficient to find the "general field" described by the joint compression and tension cone, additional data on their division (division axes) should be involved: either on belonging to different structures, or on the relative ages of the tectonic stress indicators used.

RESULTS OF STRUCTURAL DATA PROCESSING

Semisam Anticline

The detailed data were collected within the limits of Abrau Peninsula and its central folded structure of the Semisam anticline striking in the northwestern (WNW–ESE) direction. In diagrams constructed on the basis of our measurements at the limbs and the axial part of this anticline, large maxima of normal faults (dip azimuth is 320°∠70°–80°) and detachments (320°∠80°) were detected. A typical case of structural paragenesis is shown in Fig. 2, where gentle slickenside surfaces with clearly expressed normal-fault kinematics are combined with detachments filled with calcite (up to 5 cm wide) and with ruptures (up to 3–4 cm wide). The orientation of detachment systems within the limits of the entire anticline is illustrated in Fig. 3. It can be seen that most detachment systems are characterized by northeastern strike, with subvertical dipping angles. This orientation of detachments corresponds to the subhorizontal orientation of the axis of maximum deviatory tension (σ_1) in the NW–SE direction. At the northwestern and southeastern periclines of the fold, the detachment systems are slightly shifted to the NNE and ENE orientations, respectively, agreeing with the general turn of the structure. At some points, we found a multistage character of northwestern tension; it can be identified from different generations of mineral filling of the detachment faults investigated during field studies. Here we can distinguish at least three episodes of mineral-filling growth in this detachment fault. The mineral filling of these generations is represented by (a) white massive calcite, (b) transparent fine-crystalline calcite, and (c) yellowish large-crystalline calcite forming rounded concretions 10 cm in size on the earlier detachment druses. A superposed regime with a northeastern (NE 70°) orientation of the axis of maximum deviatory stress and represented by NW-striking detachment systems was reported at a considerably smaller number of observation points. When validating its relative age, we relied on the fact that detachment systems with this direction disturb the earlier tectonic parageneses of both the fractures and detachment faults [10].

For the studied area, most of the measured slickenside surfaces with structural–kinematic data are normal faults; reverse faults and thrusts are twice as rare. Left- and right-lateral strike-slips comprise about one third of the number of normal faults. Based on the reconstruction of tectonic stresses using cataclastic analysis in different parts of the Semisam anticline, we discovered considerable variability in the orientations of the principal stress axes and the types of stress state. The reconstructed axes of main compression stresses (σ_3) have two main orientations: subhorizontal northeastern (NE 50°–SE 230°) and nearly vertical (with a small northeast or southwest inclination). The axes of intermediate compression stresses (σ_2) are characterized by a position with dip azimuths NE 50° ∠25°–45° and SE 145° ∠10°–30°, while the axis of minimum compression stresses (σ_1) is oriented subhorizontally and in the northwestern direction (NW 320°). For majority of the observation points, the values of the Lode–Nadai factor are nearly zero (from –0.15 to +0.15), and this corresponds to a stressed state of a pure or simple strike-slip. Note that the earlier studied parts of the Semisam anticline are characterized by variations and change in position ("reindexing") of the maximum compression and the intermediate axes (σ_3 and σ_2, respectively), while the orientation of the axis of deviatory tension (σ_1) is chiefly unchanged and NW–SE-directed (see Fig. 3). The detailed distribution of the

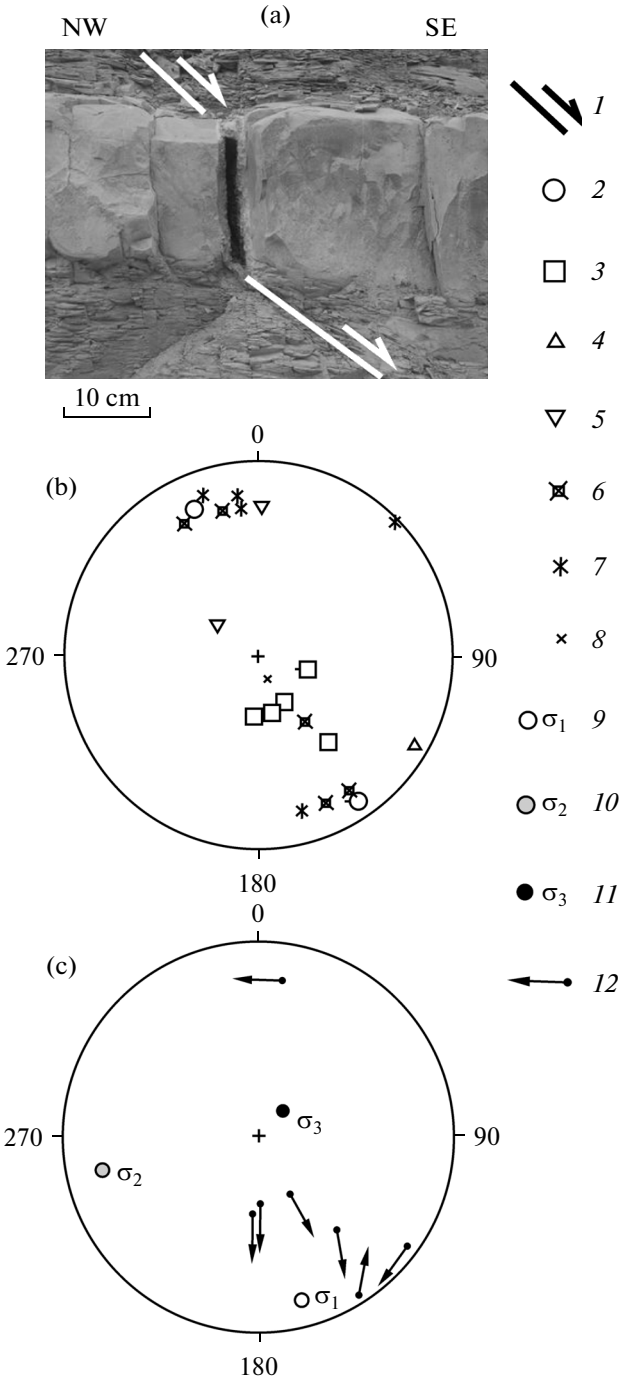

Fig. 2. Normal faulting-and-detachment parageneses in the near-axial part of the Semisam anticline (obs. point 11633). (a) NE-trending detachment paragenetically related to the slickenside surfaces of normal faulting kinematics; (b) and (c) are the radial charts (stereographic projection to the upper hemisphere) with the poles of tectonic crack planes of different types (b) and with the positions of principal stress axes determined by cataclastic analysis (c). (*1*) directions of relative slips of fault walls; (*2*)–(*7*) poles of tectonic cracks with the dominating slip types: (*2*) reverse faults, (*3*) normal faults, (*4*) right-lateral strike slips, (*5*) left-lateral strike slips, (*6*) detachments, (*7*) veins; (*8*) dip and strike of bedding (normal); (*9*)–(*11*) orientations of the axes of main normal stresses: (*9*) minimum (tension), (*10*) intermediate, (*11*) maximum (compression); (*12*) slip direction of the hanging wall in the poles of tectonic cracks with structural–kinematic data (slickenside surfaces) being used in reconstruction.

reconstructed orientations of the principal stress axes and stress state settings are given in publication [10], devoted to tectonophysical research of this folded structure.

The obtained data allow us to establish structural paragenesis within the limits of the Semisam anticline; this paragenesis is related to northwest-oriented (NW 320°) subhorizontal deviatory tension and is traced by the detachment and normal-fault systems of a northeastern direction. This deformation type may be characteristic for the larger (regional) scale as well.

The portion of the northeast-directed Sukko River valley and other fine valleys of the same direction were probably formed in large zones where detachment (diverging) deformations concentrated. In the vicinity of these valleys, we noticed an increase in the concentration of detachment structures.

The Data on Recent Stress State at the Western Pericline of Greater Caucasus

In addition to the Semisam anticline, we studied the closely located structures of the Semigorskaya anticline and the Kerch–Taman transverse trough. The northern limb of the Semigorskaya anticline (composed by the rhythmic interleaving of mostly carbonate Turonian–Coniacian rocks) was studied at the open pit located in the Neberdzhai River valley. Here, at two adjacent points, we reconstructed essentially different local stress states (table). In one case, the horizontal shortening setting with a submeridional maximum compression axis (σ_3) and a subvertical maximum deviatory tension axis (σ_1) was observed. In another case, the reconstructed setting was horizontal tension with the subvertical maximum compression axis (σ_3) and the submeridional intermediate one (σ_2). The strike and dip at both observation points are quite gentle, so we can suppose variations in the paleostress field (reindexing of the axes σ_3 and σ_2) within the rock massif. In addition to the detachment systems of northeastern and northwestern strikes, we noticed a submeridional system of detachments with small pyrite inclusions. We have not found reliable relative chronological data for these structures. We also observed detachment systems of a northeastern strike in the areas to the east in the Abin River valley and in the Upper Cretaceous deposits composing the Kotsekhuri syncline.

Within the limits of the Kerch–Taman transverse trough, which is composed of Neogene–Quaternary deposits, we studied the sites of Dzhiginka, Blagoveshchenskaya, Artyusheko settlements, the Tizdar mud volcano, Cape Zhelezhyi Rog, and Cape Kamennyi.

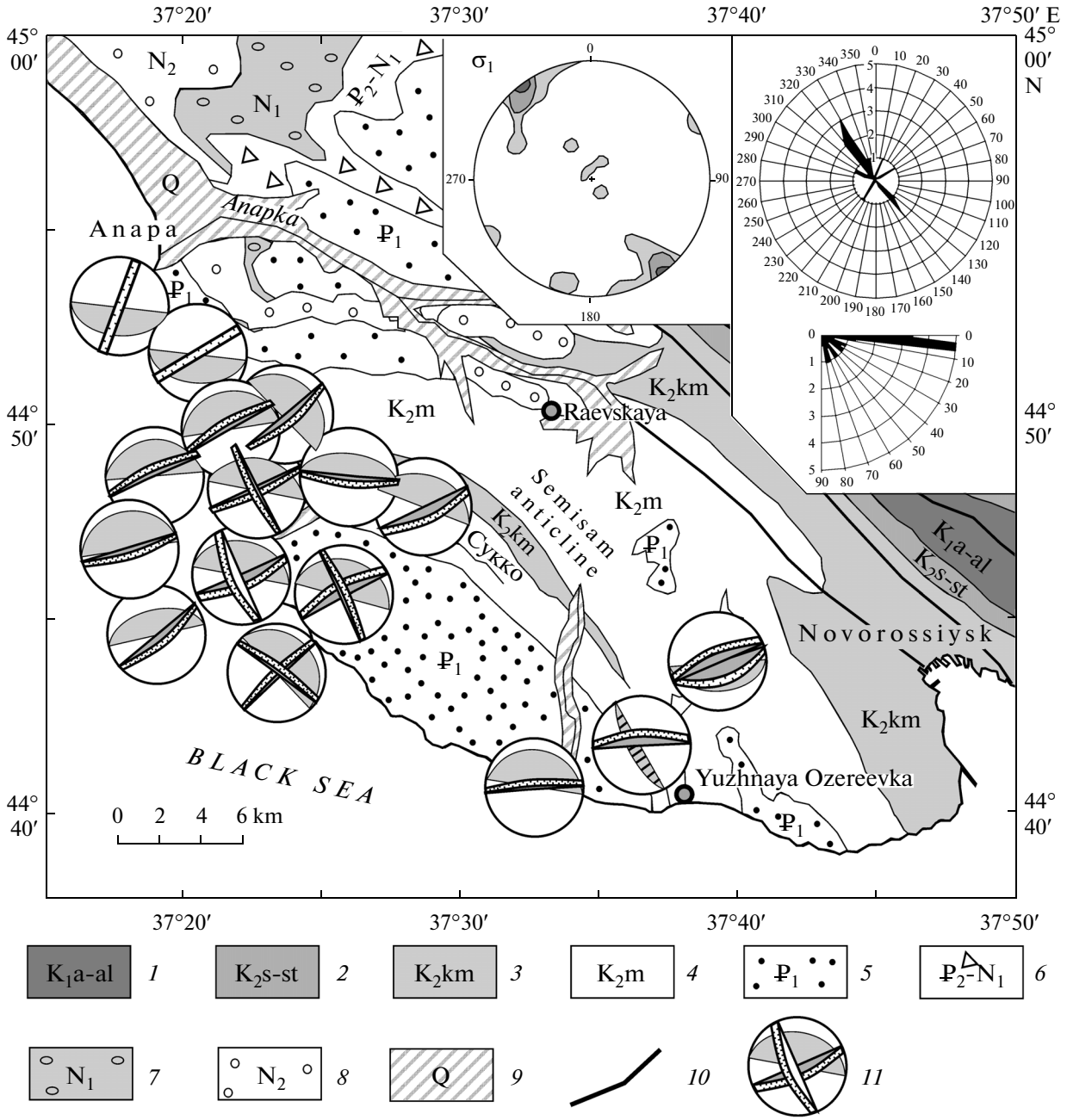

Fig. 3. The geologic scheme of the Semisam anticline area, constructed on the basis of information from [24], with the detachment systems identified during the studies. (*1*)–(*9*) deposits: (*1*) Aptian–Albian, (*2*) Cenomanian–Santonian, (*3*) Campanian, (*4*) Maastrichtian, (*5*) Paleocene, (*6*) Eocene–Maikopian, (*7*) Miocene, (*8*) Pliocene, (*9*) Quaternary; (*10*) faults; (*11*) radial charts (stereographic projection to the upper hemisphere) showing strikes and dips (double lines with tick marks) and bedding (light-gray filling) of the revealed detachment systems at the observation points. In left inset, the distribution density for outcrops of the axes of maximum deviatory tension (σ_1) calculated by using cataclastic analysis on fractures with the revealed slip character. Right inset, the same data in the form of rose diagrams of dipping azimuths (top) and inclination angles (bottom) for the σ_1 axes. The numbers denote amount of points with determined local stress tensors with the step of 10° for dipping azimuths and 5° for dipping angles.

Only fractures were measured at all points, while representative values of kinematic paleostress indicators (slickenside surfaces, detachments, etc.) could not be measured. A few structures found here were represented by small-amplitude displacements showing strike-slip and/or normal faulting motions. In general, the degree of rock alteration under the effect of tectonic and gravity stresses is smaller here, compared to the folded structure; therefore, slickenside surfaces, detachments, and other kinematic indicators are almost absent here. However, valid data on geological indicators of paleostresses were obtained for the

Parameters of the paleostress state at the western pericline of the Greater Caucasus

Tectonic structure	Nos. of obs. points	Coordinates of observation points		Age of deposits	Strike and dip		σ_1		σ_2		σ_3		Type of stress state	μ_σ	Stage	α
		N	E		Dip Az.	∟	Dip Az.	∟	Dip Az.	∟	Dip Az.	∟				
Semisam anticline	11638	44°47.46′	37°54.87′	Turon.–Coniac	75	18	290	23	186	25	57	55	Horizonal tension	–0.12	1	23
	11639–11640	44°47.70′	37°54.92′	Turon.–Coniac	135	25	310	51	75	25	179	28	Horizonal compression	0.05	1	33
SE part of the Semisam anticline	11605	44°42.23′	37°36.01′	Danian	65	60 її.	17	6	285	26	118	63	Horizonal tension	–0.19	1	25
	11607–11608	44°44.23′	37°35.72′	Maastrichtian	35	25	300	35	53	30	172	41	Horizonal tension	0.52	1	46
	11609	44°43.70′	37°35.71′	Maastrichtian	145	20	60	0	330	44	150	46	Horizonal tension w/shear	–0.29	1	30
	11613	44°43.03′	37°38.79′	Maastrichtian	355	30	342	0	72	13	252	77	Horizonal tension	0.11	1	12
SW limb of the Semisam anticline	11621	44°45.10′	37°24.10′	Paleogene	195	15	135	82	318	9	228	0	Horizonal compression	–0.01	1	29
	11626	44°46.85′	37°22.96′	Danian	165	35	334	77	150	13	240	1	Horizonal compression	–0.03	1	26
Near-axial part of the Semisam anticline (*obs. point 11630 is superposed fold*)	11604	44°46.90′	37°22.98′	Danian	190	19	138	6	231	30	39	60	Horizonal tension	–0.28	1	37
	11614	44°47.22′	37°22.62′	Maastrichtian	190	20	318	6	51	25	217	64	Horizonal tension	–0.16	1	37
	11630a	44°47.45′	37°22.51′	Maastrichtian	215	42	295	18	48	51	193	33	Horizonal shear	–0.05	1	8
	11630b	44°47.45′	37°22.51′	Maastrichtian	220	85	328	54	144	36	235	2	Horizonal compression w/shear	0.14	1	38
	11631–11632	44°47.60′	37°22.40′	Maastrichtian	135	10	138	6	229	4	355	83	Horizonal tension	–0.06	1	38
	11627–11629	44°48.05′	37°22.01′	Maastrichtian	225	15	348	0	78	0	270	89	Horizonal tension	0.15	1	18
	11633–11634	44°47.71′	37°22.33′	Maastrichtian	170	15	324	6	60	44	228	46	Horizonal tension w/shear	–0.50	1	18
NE limb of the Semisam anticline	11624	44°52.13′	37°19.19′	Maastrichtian	5	30	213	69	350	16	84	14	Horizonal compression	0.04	1	16
	11623	44°52.60′	37°18.64′	Paleogene	5	30	326	26	208	44	76	35	Horizonal shear	0.15	1	46
SE side of the Kerch–Taman trough	11641	45°01.74′	37°37.66′	Miocene	30	10	11	22	102	2	197	68	Horizonal tension	0.38	1	16
	11643–11644	45°03.94′	37°32.32′	Miocene	340	15	324	6	233	18	72	71	Horizonal tension	0	1	31
	11645–11646	45°05.55′	37°26.84′	Neogene	35	3	233	11	139	22	348	65	Horizonal tension	0.01	A	33
	11645–11646	45°05.55′	37°26.84′	Neogene	35	3	321	50	57	5	151	40	Shear in vertical plane	–0.04	B	13

The first column denotes the tectonic structure, within which the observation point is located. Other columns present the data on numbers and coordinates of observation points; age of deposits; strike and dip of bedding (regular in all points, except obs. point 11605 where it is overturned); the orientations of the principal stress axes (σ_1 is the minimum (deviatory tension), σ_2 is the intermediate, and σ_3 is the maximum compression) reconstructed by cataclastic analysis [23] from structural–kinematic data on ruptures; type (setting) of the stress state; Lode–Nadai factor μ_σ; number of deformation stages; and angle α (between the slip direction on the rupture plane and the direction of tangential stresses acting on the same plane).

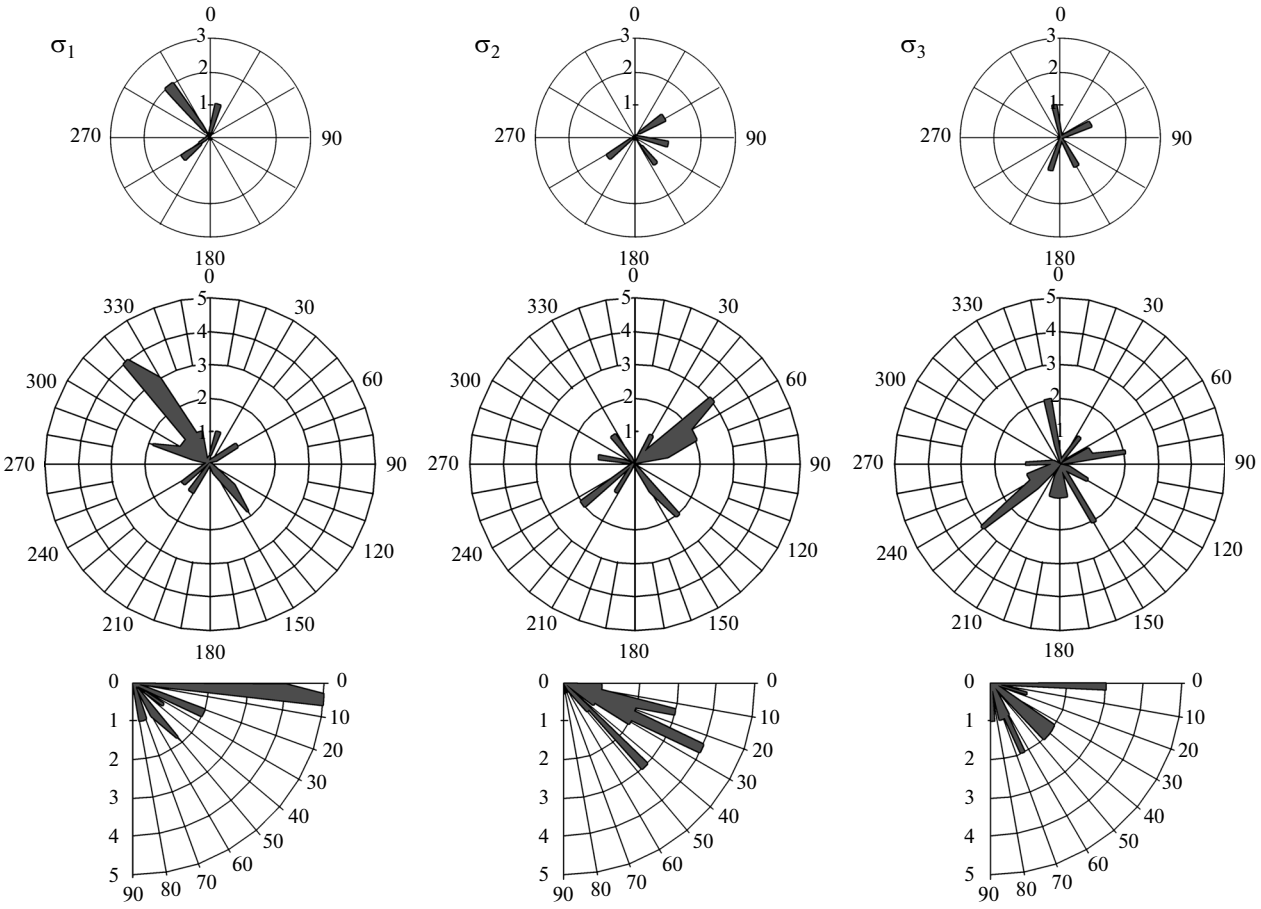

Fig. 4. Radial charts showing orientations of the reconstructed axes of principal stresses at the western pericline of the Greater Caucasus. The upper row is constructed on the basis of data collected in the young (Neogene) deposits; the middle and lower ones generalize all the obtained data. The middle and upper rows show the dip azimuths of the principal stress axes: σ_1, minimum compression (deviatory tension); σ_2, intermediate; and σ_3, maximum compression stresses. The lower row represents the dip angles of the respective axes. The charts illustrate the number of points with the determined local stress tensors with a step of 10° for dipping azimuths and 5° for dipping angles.

southeastern side of the trough, at the open pits near Shkol'nyi, Fadeevo, and Yurovka settlements (observation points nos. 11641–11646, see table). At all observation points in the gently dipping Miocene–Pliocene deposits cataclastic analysis revealed horizontal tension conditions (subvertical axis of maximum compressing stresses); at one point, near the Yurovka settlement, vertical shear conditions (with the resulted cutting fault-like deformation) were also determined. In the open pit near Shkol'nyi settlement, the most widespread are submeridionally striking detachment structures, while west–northwest-striking structures are less abundant.

General Results of Reconstruction

Reconstruction results at all observation points at the western pericline of Northwestern Caucasus are generalized in the table, in radial charts (Fig. 4), and in stereograms (Fig. 5) and represent the most typical orientations of the principal stress axes. The detected with higher confidence is the axis of deviatory stress (σ_1): it is oriented in NW–SE direction in a horizontal position (dipping azimuth is 325° ∠0°). Other determined positions of σ_1 axes do not form significant maxima, but also stretch along the NW–SE direction. For the axes of main compressing stresses (σ_3), subvertical positions with peaks at dipping azimuths of SW 230° ∠60°, SW 230° ∠89°, and NE 50° ∠60° are characteristic. Most subhorizontal orientations of σ_3 axes dip in a northeastern direction (the dipping azimuth is NE 55° ∠0°). The north–northwestern orientation (SE 150° ∠40°) of σ_3 axis is characteristic chiefly for the observation points located at the southeastern side of the Kerch–Taman trough. The intermediate (σ_2) axis forms two maxima: the dipping azimuths of NE 75° ∠20° and SE 145° ∠25°. The defined orientations of the σ_2 axis can often be found for the vertical orientation of the axis of maximum compressing stresses (σ_3).

The predominant orientations of the principal stress axes obtained from structural–kinematic data

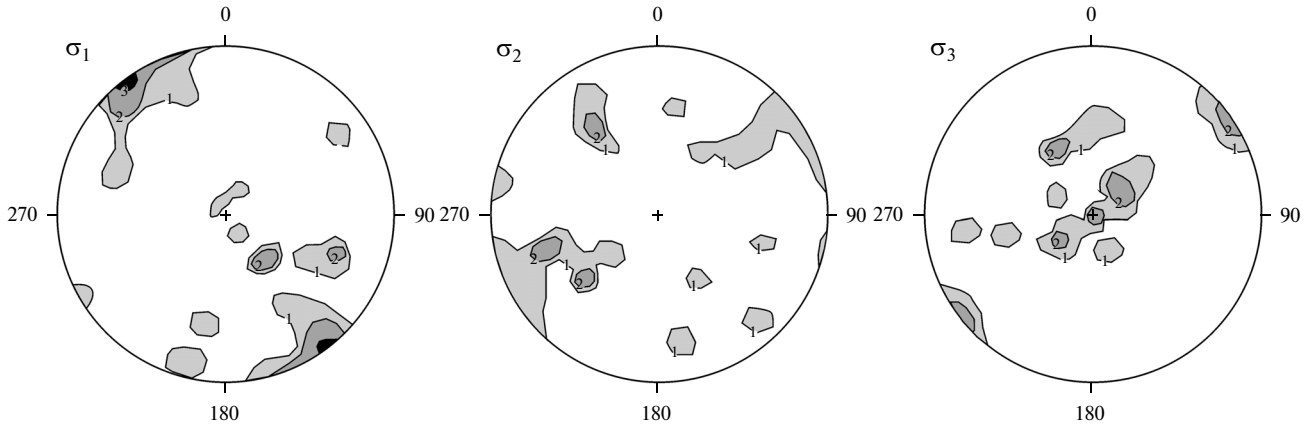

Fig. 5. Radial charts (stereographic projection to the upper hemisphere) for reconstructed axes of principal stresses at the western pericline of the Greater Caucasus (pole density distribution from outcrop data are shown): σ_1, minimum compression (deviatory tension); σ_2, intermediate; and σ_3, maximum compression stresses.

on fractures are close to the orientations of the *T* and *P* axes of particular sources of earthquakes recently recorded in this area (see Fig. 1). Based on USGS data [36], the Novokubanskoe earthquake of November 9, 2002 occurring near Bezvodnyi settlement (18 km northwest of Krymsk and 40 km northeast of Anapa) had an axis of compression stresses dipping northeast at 45° and an axis of tension dipping southwest at 224° ∠45°. Based on the Information Processing Center of the Geophysical Survey, Russian Academy of Sciences [37], the Anapa earthquake of December 10, 2012 had an axis of compression stresses oriented to southwest (227° ∠28°) and a tension axis oriented to northwest (334° ∠28°). Thus, the focal mechanisms of these two earthquakes have compression axes oriented northeast-southwest. However, these data are insufficient to make a valid comparison between them and our tectonophysical field results.

The positions of axes of maximum compression (σ_3) and maximum deviatory tension (σ_1), reconstructed by cataclastic analysis for the local stress states of the western pericline of Greater Caucasus and analyzed in the charts (Figs. 4 and 5), do not give a clear view of the possible united strain regime due to the considerable variations of both orientations of the principal stress axes and the types of stress state. In the chart shown in Fig. 6a, axes σ_3 and σ_1 of different local stress states have steep dip values (and close to each other) indicating a distribution of settings with different types of stress state in the studied area: both horizontal compression and horizontal tension. Obviously, this complicates the task of finding the general version of the regional stress field. But if we make a formal subdivision of local stress states on dipping angle of the axis into dips less than 45° and more than 45°, we can obtain two versions satisfying the principle of finding the regional "general field" of stresses by the technique from [26]. The first version (Fig. 6b) is characterized by the setting of a horizontal compression with a subhorizontal northeastern maximum compression and a steep deviatory tension: σ_3 axis has a dipping azimuth of 65° ∠12°; σ_1 axis, 315° ∠60°. The planes of maximum tangential stresses have the dipping azimuths of 90° ∠62° (submeridional right-lateral strike-slip with a reverse fault component) and 214° ∠44° (left-lateral strike-slip with a reverse fault component). Based on study of the tectonic fractures and fine rupture systems, the submeridional right-lateral strike-slips are the most widespread in the entire Northwestern Caucasus [11]. Among the fault systems, the left-lateral displacements are in a greater degree characterized by a latitudinal orientation, compared to the solution inferred from the "general" regional field. It should be noted that four tilted compression axes in a NW (to NNW) direction have not been included in the compression cone in Fig 6b; these axes reflect the result of "reindexing" the σ_2 and σ_3 axes for some local stress states. The intermediate (σ_2) axes of these stress states are marked with triangles in the compression cone. The second version is represented by the setting of horizontal tension and characterized by steep dipping of the maximum compression axis (σ_3, dipping azimuth is 170° ∠80°), and by tahe subhorizontal northwest-oriented axis of maximum deviatory tension (σ_1, dipping azimuth is 333° ∠10°). The planes of maximum tangential stresses have dipping azimuths of 145° ∠35° (normal fault) and 335° ∠55° (normal fault). However, the considered solutions probably represent sequential changes of the united stress field over time. They are, in fact, spatial versions of elongation on the fault zones of different scales, both along the axis of the folded structure and in the vertical direction (from the "mountain roots" to the rising mountain tops). Signs of tectonic flow of the material along the axis of folded structure and in a subvertical direction under collision (converging) settings are noticed in some publications [21, 22]. The results of

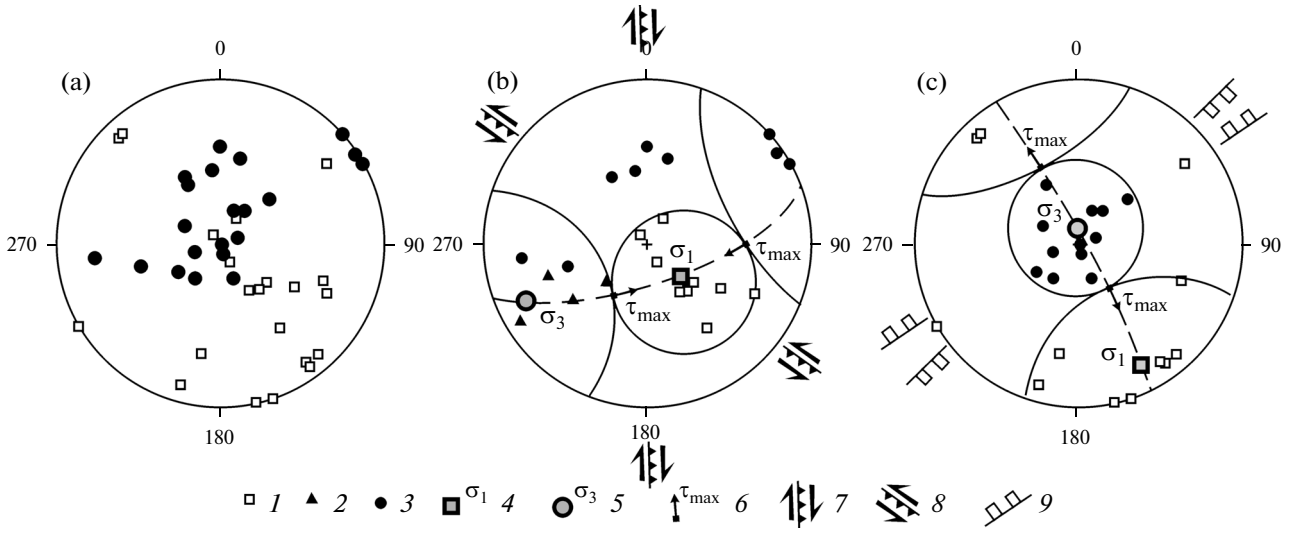

Fig. 6. The positions of the reconstructed axes of principal stresses (stereographic projection to the upper hemisphere): (a) for all reconstructed local stress states; (b) for the group of local stress states formed under horizontal compression; (c) for the group of local stress states formed under horizontal tension. (*1*)–(*5*) axes of main normal stresses: (*1*) minimum compression σ_1 (deviatory tension), (*2*) intermediate σ_2 (for local stress states having submeridionally dipping σ_3 axes), (*3*) maximum compression σ_3 (deviatory compression), (*4*) and (*5*) σ_1 and σ_3 for the groups of local stress states, respectively; (*6*) poles of the planes of maximum tangential stresses (arrow indicates the direction of hanging wall motion); (*7*)–(*9*) strike and kinematic type of faults that may form under the given setting: (*7*) right-lateral oblique faults (strike-slip and reverse fault), (*8*) right-lateral oblique faults (strike-slip and reverse fault), (*9*) normal faults.

our detailed research also agree with structural data obtained for the entire Caucasus, indicating the longitudinal elongation of the folded structure on the systems of lateral faults (strike-slips) [7].

GEODYNAMICAL INTERPRETATION OF THE OBTAINED RESULTS

There are several versions of how the field data results can be interpreted. First, let us consider the multiple detachments and normal faults noticed in the stress field. To interpret the emplacement settings of these structures, two scenarios are proposed that do not contradict, but mutually supplement, each other, clearly marking the role played by the leading factor. The first scenario was considered in [11]; it implies that multiple normal faults and detachments are surface manifestations of the SW–NE-trending Anapa and Dzhiginka flexure-fault zones. The folded structures of the Northwestern Caucasus suffer a flexure-like bend here; west of this bend, they dip and become covered with Late Cenozoic deposits of the Kerch–Taman transverse trough. However, this scenario contradicts the orientation of the detachments structures revealed by our study according to which the detachment structures are directly related to the position in the studied Semisam anticline. Additionally, the found orientations of the axes of maximum deviatory tension in the periclinal parts of the fold differ from the NW–SE trend, which dominates in other parts of this structure. It would be more appropriate to consider a larger area located at the boundary between the folded structure and the transverse trough. Widespread normal-fault and detachment parageneses, including the mentioned SW–NE-trending flexure-fault zones, are caused by the transitional character of this area. In this part of the dipping folded structures of Northwestern Caucasus, settings of horizontal tension and horizontal compression dominate, while in the areas to the east the settings of horizontal compression with shear and those of horizontal shear begin to play a more significant role. Thus, in the junction between the Caucasus folded structure and the Kerch–Taman transverse trough, a zone with one geodynamical regime changes to another; in its order, this change causes the change in the type of stress state and the orientations of the principal stress axes. In the southeastern side of the trough, only the settings of horizontal tension have been established.

The second scenario is related to elongation along the axis of the folded structure and, in particular, along the axis of the large Semisam anticline. The revealed orientation of the detachment systems, slickenside surfaces, and fine ruptures, which form regular structural parageneses, directly indicates the elongation of the western termination of the Greater Caucasus in the NW–SE direction during a quasiplastic flow of rocks along the axis of the folded structure. The axis of the maximum deviatory tension found from the reconstruction data is oriented subhorizontally in the northwestern direction (NW 320°) and coincides with the strike of the main folded structures. Near the Sukko River valley, in the limb of the Semisam anticline, the counted percentage of the detachments (opened gaps and mineral filling) relative to the host

rocks along this direction (NW 320°) is about 5.5%. The small value of relative horizontal shortening in the NE–SW direction (from 6 to 25%), calculated in some publications [4, 11, 31] for this area, is comparable to the NW–SE elongation.

The distribution of the cutting detachment systems, which are related to the superposed regime with a northeastern (NE 70°) orientation of the σ_1 axis, can also be explained differently on the basis of the earlier studies [11, 35]. At first, this can be caused by the collapse of the Greater Caucasus mountain structure after its uplift above the Black Sea Basin and the West Kuban trough. The second possible explanation implies that this tension is related to the NNW compression, which is clearly manifested in Miocene deposits. However, within the limits of the Semisam anticline, this direction of compression stresses has not been reliably verified. Probably, at the moment when the later NNW compression manifested, the area of the Abrau Peninsula was quite a "rigid" block, and therefore the influence of later stresses can be detected only in Late Cenozoic deposits of the adjacent, "less rigid" blocks, or in the zones of the most recent ruptures. According to neotectonic reconstructions, this area belongs to the Abrau uplift of the Bakan bachyarch [14]. The north-northwestern (NNW 340°) direction of maximum compression is manifested in Miocene deposits at the western pericline of the Greater Caucasus in the zone of its transition to the structures of the Kerch–Taman and West Kuban troughs. This orientation (NNW 340°) of maximum compression stress of the superposed phase of deformation has been found independently by Russian and French research groups using two different methods [34] and is verified by the results of the calculations by the cataclastic analysis. Note that we obtained quite steep orientations of axes of maximum compression stresses, with inclination angles from 65 to 70 degrees.

Let us note, as a suggestion, the interesting regularity of spatiotemporal relations between the studied indicators. At the western pericline of the Greater Caucasus, the first (synfolding) stage was characterized by SW–NE orientations of the σ_3 and σ_2 axes, while the σ_1 axis was oriented in the NW–SE direction. Later, for the contemporary state of uplift of the mountain structure, the σ_1 axis becomes of a SW–NE orientation. We can suppose that in the Kerch-Taman zone the axes of maximum compression stresses at the stage of formation of the folded structures (this stage took place here later than in the structures of Caucasus) were oriented in the NNW–SSE direction, while the σ_1 axes were ENE–WSW-oriented. The contemporary detachment systems become ENE-oriented here, while the σ_1 axis turn to the NNW–SSE orientation. We think that the settings of horizontal tension, which are determined at the western pericline of the Greater Caucasus and referring to the superposed deformation stage (with the σ_1 axis being SW–NE-oriented), are related exclusively to the uplift and near-surface release of stresses. As a result of rising, the rock massif becomes of a higher elevation relative to the poorly compressed sediments in the adjacent troughs, and, in fact, the lateral load of this rock massif is completely released (in the case under discussion, on the sides of the Black Sea and the West Kuban trough). Under these settings, the systems of superposed northwest-trending detachments, gaps, and grabens are formed. The availability of more qualitative seismological information might clarify, first, whether the settings of northeastern compression exist in the lithosphere at the western pericline of the Greater Caucasus, and, second, whether the identified transition from the earlier (synfolding) stage to the modern one can be considered both in the temporal aspect and with respect to a change in stress state with depth.

CONCLUSIONS

When studying the folded deformations of the Greater Caucasus, main attention is usually paid to the investigation of the shortening across the folded structure. When developing the techniques for defining the horizontal shortening and when estimating the amount of shortening, possible deformations along the axis of the folded structure should be taken into consideration. Our studies show that similar deformations exist on different scales of the studied structures, and, in some cases, the value of relative elongation can be determined. The found orientation of the systems of detachments and tension fractures that form regular structural parageneses indicates the elongation of the western termination of the Greater Caucasus in the NW–SE direction during quasiplastic flow of rocks along the axis of the folded structure. According to the calculations for the western part of Northwestern Caucasus, the horizontal SW–NE-directed shortening has a small size and is quite comparable, in a percentage sense, to the NW–SE elongation calculated for a small site within the same area. The NW–SE elongation likely occurred over a long time: this is indicated by the multiphase character of the mineral filling of detachments and the revelation of local stress states in Neogene deposits having a NW–SE orientation in the deviatory tension axes.

The paleostress field, having a northwestern orientation of the axes of maximum compression stresses and being manifested particularly clearly during the main folding phase, is verified by another method (in addition to the earlier studies). Based on cataclastic analysis data, the stress field with northeastern compression dominates; also, in different sites, the settings of horizontal compression (northeastern orientation of the σ_3 axis) changes to a horizontal compression (northeastern orientation of the σ_2 axis).

The character of stress variation within the transition zone between the folded structures of Northwestern Caucasus and the transverse structures of Kerch–Taman trough is identified. The gradual mosaic

change in orientations of axes of main normal stresses allows us to understand the processes running in this transitional zone. Here the settings of horizontal compression and horizontal shear (with northeastern compression), which are predominant in the Caucasus region, change to the settings of horizontal tension with a steep dipping of the NNW-oriented axes of maximum compression.

ACKNOWLEDGMENTS

The work was supported by the Russian Foundation for Basic Research (projects nos. 12–05–10069k and 13–05–10066-k).

The authors thank their colleagues from the Schmidt Institute of Physics of the Earth, Russian Academy of Sciences, and the Moscow State University—L.M. Rastsvetaev, Yu.L. Rebetsky, T.Yu. Tveritinova, and A.V. Mikhailova—for their advice and consultations during the preparation of the manuscript.

REFERENCES

1. A. P. Afanasenkov, A. M. Nikishin, and A. N. Obukhov, *Geologic Structure and Hydrocarbon Potential of the East Black Sea Region* (Nauchn. mir, Moscow, 2007) [in Russian].
2. Ch. B. Borukaev, "On palinspastic constructions," Geotektonika, No. 6, 32–45 (1970).
3. V. A. Viginskii, Extended Abstract of Candidate's Dissertation in Geology and Mineralogy (IFZ AN SSSR, Moscow, 1986).
4. T. V. Giorgobiani and D. P. Zakaraya, *Folded Structure of Northwestern Caucasus and Mechanism of Its Formation* (Metsniereba, Tbilisi, 1989) [in Russian].
5. O. I. Gushchenko, "Kinematic principle of reconstructing the principal stress directions (based on the geological and seismological data)," Dokl. Akad. Nauk SSSR, Ser. Geofiz. **225**, 557–560 (1975).
6. A. L. Kozlov, "Coast of the Black Sea in the area of Sochi and lower stream of Mzymta River," in *Caucasus Excursion (Black Sea Coast). International Geological Congress, XVII Session* (Moscow, 1937), pp. 26–44.
7. M. L. Kopp, "Structural patterns related to longitudinal movements within fold belts," Geotektonika, No. 1, 21–36 (1991).
8. N. V. Koronovskii, L. A. Sim, and B. V. Boinagryan, "Neotectonic and contemporary fields of tectonic stresses in Caucasus with respect to seismicity," Vestn. Mosk. Gos. Univ. Ser. 4. Geol., No. 2, 3–14 (1996).
9. Yu. G. Leonov, O. I. Gushchenko, M. L. Kopp, and L. M. Rastsvetaev, "Relationship between the Late Cenozoic stresses and deformations in the Caucasian sector of the Alpine Belt and its northern foreland," Geotectonics **35**, 30–50 (2001).
10. A. V. Marinin, "Tectonophysical studies of the Semisam Anticline (Northwestern Caucasus)," Geodin. Tektonofiz. **4**, 461–484 (2013). doi: 10.5800/GT-2013-4-4-0113.
11. A. V. Marinin and L. M. Rastsvetaev, "Structural parageneses of Northwestern Caucasus," in *Problems of Tectonophysics: On the Fortieth Anniversary of Organizing the Laboratory of Tectonophysics in the Institute of Physics of the Earth, Russian Academy of Sciences* (IFZ RAN, Moscow, 2008), pp. 191–224.
12. E. E. Milanovskii and V. E. Khain, *Geologic Structure of Caucasus*, vol. 8 of *Overview of Regional Geology of the USSR* (Mosk. Gos. Univ., Moscow, 1963) [in Russian].
13. M. V. Muratov, "Overview of tectonics for the area in the vicinity of Chvizhepse mineral springs (southern slope of the Main Greater Caucasus Range)," Byull. Mosk. O-va. Ispyt. Prir., Otd. Geol. **18**, No. 2, 3–36 (1940).
14. S. A. Nesmeyanov, *Neostructural Zoning of Northwestern Caucasus* (Nedra, Moscow, 1992) [in Russian].
15. A. M. Nikishin, A. V. Ershov, and V. A. Nikishin, "Geologic history of Western Caucasus and the adjacent foredeeps based on analysis of the regional balanced section," Dokl. Earth Sci. **430**, 155–157 (2010).
16. P. N. Nikolaev, *A Method of Tectonodynamic Analysis*, Ed. by N.I. Nikolaev (Nedra, Moscow, 1992) [in Russian].
17. D. N. Osokina, "On the hierarchical properties of tectonic field of stresses and deformations in the Earth's crust," in *Fields of Stresses and Deformations in the Earth's Crust*,, Ed. by A. S. Grigor'ev and D. N. Osokina (Nauka, Moscow, 1987), pp. 136–151.
18. V. I. Popkov, "Postsedimentation character of development of intraplate dislocations as reflection of pulsed nature of deformation processes," Geodin. Tektonofiz. **4**, 327–339 (2013).
19. L. M. Rastsvetaev, "Mountain Crimea and Northern Black Sea region," in *Faults and Horizontal Movements of Mountain Structures in the USSR* (Nauka, Moscow, 1977), pp. 95–113.
20. L. M. Rastsvetaev, "Paragenetic method of structural analysis of tectonic faults," in *Problems of Structural Geology and Tectonophysics* (GIN AN SSSR, Moscow, 1987), Vol. 2, pp. 173–235 [in Russian].
21. L. M. Rastsvetaev, S. G. Korsakov, T. Yu. Tveritinova, I. N. Semenukha, and A. V. Marinin, "On some general features of structure and tectodynamics of Northwestern Caucasus," in *Problems of Geology, Mineral Resources and Environment in South Russia and Caucasus* (Novocherkassk, 1999), Vol. 1, pp. 69–73.
22. L. M. Rastsvetaev, A. V. Marinin, and T. Yu. Tveritinova, "Late-Alpine fault systems and geodynamics of the West Caucasus," Izv., Phys. Solid Earth **46**, 394–403 (2010).
23. Yu. L. Rebetsky, *Tectonic Stresses and Rigidity of Rock Massifs* (Nauka, Moscow, 2007) [in Russian].
24. V. A. Serezhenko and P. P. Kuzubov, *Geological Map of the USSR, 1 : 200 000. Caucasian Series. Sheet L-37-XXVI/XXXII* (Nedra, Moscow, 1971).
25. L. A. Sim, "A study of tectonic stresses by geological indicators (mehtods, results, recommendations)," Izv. Vyssh. Uchebn. Zaved., Geol. Razved., No. 10, 3–22 (1991).
26. L. A. Sim, "Influence of global tectogenesis on neotectonic stress state of the European cratons," in *M.V. Gzovskii and Development of Tectonophysics* (Nauka, Moscow, 2000), pp. 326–350.

27. V. E. Khain, S. L. Afanas'ev, I. B. Borukaev, and M. G. Lomize, "The main features of structural-facial zonality and tectonic history of Northwestern Caucasus," in *Geology of the Central and Western Caucasus* (Gostoptekhizdat, Moscow, 1962), Vol. 3, pp. 5–47.

28. A. N. Shardanov, "Tectonic structure of Northwestern Caucasus," Tr. Krasnodar. Fil. VNIIneft', No. 3, 6–42 (1960).

29. T. A. Shardanova and N. A. Solov'eva, "Influence of neotectonics and eustatic variations on formation of the Sarmatian, Maeotian, and Pontic deposits in the Taman Peninsula," Vestn. Mosk. Gos. Univ. Ser. 4. Geol., No. 5, 36–43 (2006).

30. A. P. Shcheglov and V. A. Chekunov, "Late orogenic stage in the tectonic evolution of the southern slope of Northwestern Caucasus (between Gelendzhik town and Abrau settlement)," in *Mechanisms of Structure-Formation in the Lithosphere with Respect to Seismicity. Abstr. All-Union Symp.* (IFZ AN SSSR, Moscow, 1991), pp. 78–79.

31. F. L. Yakovlev, "The first version of 3D model of the sedimentary cover structure in Northwestern Caucasus based on the field of folded deformations," in *Problems of Tectonophysics: On the Fortieth Anniversary of Organizing the Laboratory of Tectonophysics in the Institute of Physics of the Earth, Russian Academy of Sciences* (IFZ RAN, Moscow, 2008), pp. 335–345.

32. F. L. Yakovlev, "Tectonophysical methods of studying the structures of linear folding," *Modern Tectonophysics. Methods and results. Proceedings of the First Workshop for Young Scientists* (IFZ RAN, Moscow, 2009), pp. 318–347.

33. J. Angelier, "Determination of mean principal directions of stresses for a given fault population," Tectonophysics **56**, 17–26 (1979).

34. A. V. Marinin and A. Saintot, "Comparison of methods to reconstruct paleostress regimes in the NW-Greater Caucasus fold-and-thrust belt," C. R. Geosci. **344**, 181–190 (2012).

35. A. Saintot and J. Angelier, "Tectonic paleostress fields and structural evolution of the NW-Caucasus fold-and-thrust belt from Late Cretaceous to Quaternary," Tectonophysics **357**, 1–31 (2002). doi: 10.1016/j.crte.2012.01.004

36. M5.5 southwestern Russia earthquake's Centroid Moment Tensor, US Geological Survey. http://earthquake.usgs.gov/earthquakes/eventpage/usp000bh4m#scientific_tensor:us_gcmt20021109021811

37. Data on 10 earthquakes recorded by the Emergency Report Service, Geophysical Survey of the Russian Academy of Sciences. www.ceme.gsras.ru/cgi-bin/info_quake.pl?mode=1&id=200

Reviewers: V.G. Trifonov, M.L. Kopp
Translated by N. Astafiev